Chapter 7
Signal, Image Processing, and Machine Learning: The Key to Complex Problems in Medicine and Biology

Mahsa Zahery and Kayvan Najarian

Introduction

Computer-aided decision-making systems have been introduced into many fields, such as economics, medicine, architecture, and agriculture. The increasing demand and rapid pace of development of such computer-aided decision-making systems displays their popularity and success in aiding and enhancing various fields. In the field of medicine, the advantage of having such systems is in the expense, labor, energy, and budget savings they provide to the health care environments. In the following sections, a brief description of the application of such systems in hemorrhagic shock, attention detection, traumatic brain injuries, and pelvic fracture detection has been provided. A flowchart of the procedure of developing such systems is represented in Fig. 7.1.

Hemorrhage Detection

An example of using a computer-aided decision-making system is in dealing with traumatic injuries (injuries caused by an accident, a battle, or an illness) wherein the effective decisions produced by a computer-aided system can be very handy in controlling the situation and quickly assessing the patient's health condition. Such systems are typically designed to detect the type of illness, assess the severity, and thereby help in the allocation of resources.

In [11], a computational system is proposed, which is designed to estimate the severity of blood volume loss. Severe hemorrhage is the event of losing large volumes of blood which leads to reduced blood and oxygen perfusion to vital

Mahsa Zahery (✉) • Kayvan Najarian
Department of Computer Science, Virginia Commonwealth University, Richmond, VA, USA
e-mail: zaherym@vcu.edu; knajarian@vcu.edu

B. Toni (ed.), *Advances in Interdisciplinary Mathematical Research*, Springer Proceedings in Mathematics & Statistics 37, DOI 10.1007/978-1-4614-6345-0_7,

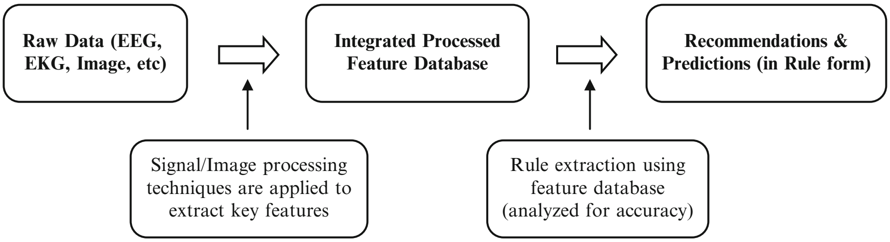

Fig. 7.1 Procedure of developing a computer-assisted system using signal processing and machine learning [3]

organs. This can be life-threatening and hence requires immediate care and attention. Depending on the severity, hemorrhage can be categorized into different levels, such as mild, moderate, and severe. The proposed system is capable of estimating and incorporating the severity of blood volume loss and hemorrhage knowledge. This is very efficient not only in saving lives but also in reducing the cost of treatments.

The methodology can be introduced in three steps, each of which contains novel and transformative concepts. Preprocessing of the raw signals is the first step which includes algorithms to detect QRS complex and systolic/diastolic waveforms along with the usage of an adaptive filtering method to filter the noise in the signals. The second step involves combining the features which are extracted from time domain, frequency domain, nonlinear analysis, and multi-model analysis (feature extraction step). This way, a better representation of the hemorrhage patterns is provided. The last step uses a machine learning algorithm for high-accuracy and real-time decision-making. At this stage, a new version of error-correcting output code (ECOC) has been developed. Accuracy obtained by the proposed system is much higher compared to the accuracy from the United States Army Institute of Surgical Research lower body negative pressure (USAISR LBNP) dataset thereby justifying the reliability of the proposed system (an accuracy of 99.89% in case of QRS detection and 99.95% in case of systole and diastole detection). In the following section, the conventional ECOC algorithm, as well as the properties of its improved version, is explained briefly.

Error-Correcting Output Codes (ECOC)

Combining the output of binary classifiers, ECOC [8] solves multiclass learning problems by using an error-correcting output code matrix. The framework of this method is given in Fig. 7.2.

A matrix of k rows and n columns is generated, with k representing the number of classes and n not being limited to any value as long as it satisfies the $n > \log_2 k$. Matrix elements are either 1 or -1 which are the binary codes adjusted to each class label.

The training stage of an ECOC classifier builds the coding matrix of size k by $n$following the steps provided below:

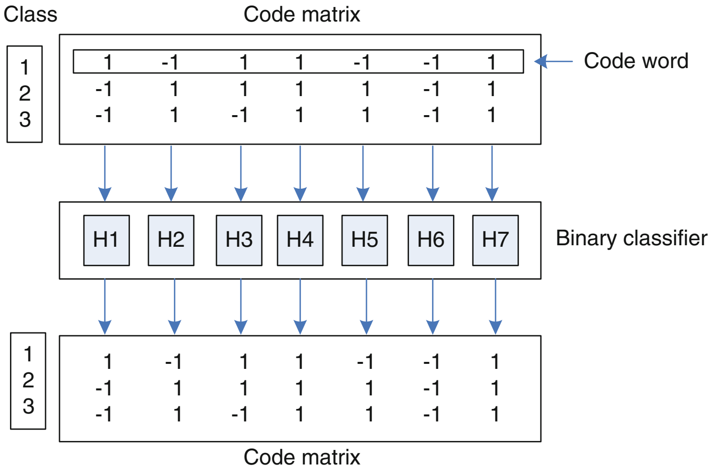

Fig. 7.2 Framework of ECOC algorithm [10]

- A coding matrix of values $1/-1$ is generated.
- For each column j of this matrix:
  - Two superclasses are made. One has all the labels i(the row numbers) for which the (ij)th element of the matrix is 1, and the other consists of the labels for -1 elements of the matrix.
  - A binary classifier is generated to differentiate between the superclasses made in the previous step.

The testing stage of the algorithm classifies a new example, given the matrix constructed at the training stage, using the following steps:

- For each column j of the matrix:
  - The probability with which the binary classifier for column j allocates the new example to label 1 superclass is calculated.
- The proximity (according to Hamming distance) of the vector containing the probabilities from all the binary classifiers (each column has one binary classifier) to each row of the matrix is calculated.
- The row giving the minimum value is the class label for the new example.

The proposed framework for ECOC in [11] improves the conventional ECOC algorithm in the following areas:

- It changes the code matrix to BCH [15] which is a specific type of error-correcting output code and is one of the most common used approaches. The choice of the code matrix is avoided in BCH, but this does not affect its error-correcting capability.
- It makes use of support vector machine (SVM) as binary classifier. SVM can handle data/sample imbalance and small sample size problems more effectively.

– It decomposes the learning problem, in the sense that by assuming a normal distribution for the data, data points in one class form several normal distributions with different expectations and standard deviations, distinguishing them from each other, while these different subclasses are still under the coverage of the same class. Afterwards, the data is allocated to different layers in each of which the region is decomposed to two subregions: one with high confidence on the prediction result and the other with low confidence. Next, the dataset is sent to the next layer for classification.

For the details on the framework of the improved ECOC algorithm, the reader is encouraged to refer to [11].

Attention Detection

With the stressful environments, extended work hours, and high workload, the high-paced life of most people has made sleep disorders a more commonplace in societies. In addition, there are certain daily tasks which are repetitive and tedious in nature, thus leading to fluctuations in people's attention spans and capacity. This is a very critical problem since losing attention during certain activities or profession can be very dangerous and deadly.

Using ECG (electrocardiograph) which is a fundamental physiological signal, a real-time monitoring system has been developed in [3] to predict whether an individual is paying attention during a task execution or not. The aim of this study is to find the effect of the body's physiological parameters on the individuals' attention level. Using noninvasive portable monitors, these signals are collected to predict an individual's inclination to sleep or loss of attention well ahead of time. With advanced signal processing techniques, informative features are extracted. Specific features related to heart's rhythm are extracted using a QRS complex detection algorithm. Next, using dual-tree complex wavelet transform (DT-CWT) and Stockwell transform, the ECG signal is decomposed to extract more features which are informative in differentiating the subtle changes in the acquired ECG signal [2] and [4]. The next step involves using machine learning algorithms to categorize these extracted features between cases of attention and non-attention. Finally, EEG (electroencephalograph) signals are analyzed and classified to act as a benchmark for comparison with ECG classification, since EEG signals are fundamentally more informative in providing information regarding human cognitive activity [5]. However, typically EEG signal collection devices are cumbersome and many times non-portable thereby limiting its usability in real-world scenarios.

ECG and EEG signals of around 15 subjects are collected. The volunteers are asked to view videos for 40 min, consisting of 20 min of interesting clips and 20 min of clips that are not interesting. After decomposing the acquired data and analyzing it for feature extraction and classification, a fairly reasonable accuracy of 78.27% shows that with only the ECG signals of the volunteers, it is possible to distinguish between the presence and lack of attention in the subjects [5].

Dual-Tree Complex Wavelet Transform

Wavelet transform was developed to overcome the deficiencies of short-time Fourier transform (STFT). Regular Fourier transform is not always able to represent a signal's time-dependent nature. The problem is that Fourier transform does not reflect the time at which a frequency exists. This is not a problem for stationary signals. However, for nonstationary signals, STFT was introduced. STFT moves a window throughout the signal. Fourier transform is then applied to each window to obtain the frequency information of each window. The problem with STFT is that it considers the same resolution for all frequencies.

To tackle this problem, wavelet transform was developed. Wavelet transform considers different resolutions for different frequencies. Discrete wavelet transform (DWT) substitutes the infinitely fluctuating sinusoidal basis functions of Fourier transform with locally fluctuating basis functions referred to as wavelets. Wavelets are basis functions with concentrated energy using which the signals are decomposed.

Dual-tree complex wavelet transform (DT-CWT) was proposed by [9] to come up with solutions to the constraints of DWT. DWT operates a decimation task while transforming a signal. This makes DWT a shift variant transformation which creates various output wavelet coefficients in response to a small shift in the analyzed signal. The other deficiencies of DWT are susceptibility to aliasing, oscillations, and lack of directionality [7, 9], and [12].

Providing directional wavelets, shift-invariant property, as well as amending angular resolution, DT-CWT uses a dual tree of real filters to achieve the real and imaginary parts of the generated complex coefficients [13]. Figures 7.3 and 7.4 illustrate the analysis and synthesis filter banks, respectively.

Consisting of two parallel wavelet transforms, DT-CWT calculates the wavelet coefficients and scaling coefficients of the first tree in the following manner:

$$d_l^{Re}(k) = 2^{l/2}\int_{-\infty}^{+\infty} x(t)\psi_h(2^l t-k)dt,\ l=1,\ldots,j \tag{1}$$

$$c_j^{Re}(k) = 2^{j/2}\int_{-\infty}^{+\infty} x(t)\phi_h(2^j t-k)dt \tag{2}$$

where l is the scaling factor and $j$is the maximum scale. The coefficients of the second tree are calculated in similar manner:

$$d_l^{Im}(k) = 2^{l/2}\int_{-\infty}^{+\infty} x(t)\psi_g(2^l t-k)dt,\ l=1,\ldots,j \tag{3}$$

$$c_j^{Im}(k) = 2^{j/2}\int_{-\infty}^{+\infty} x(t)\phi_g(2^j t-k)dt \tag{4}$$

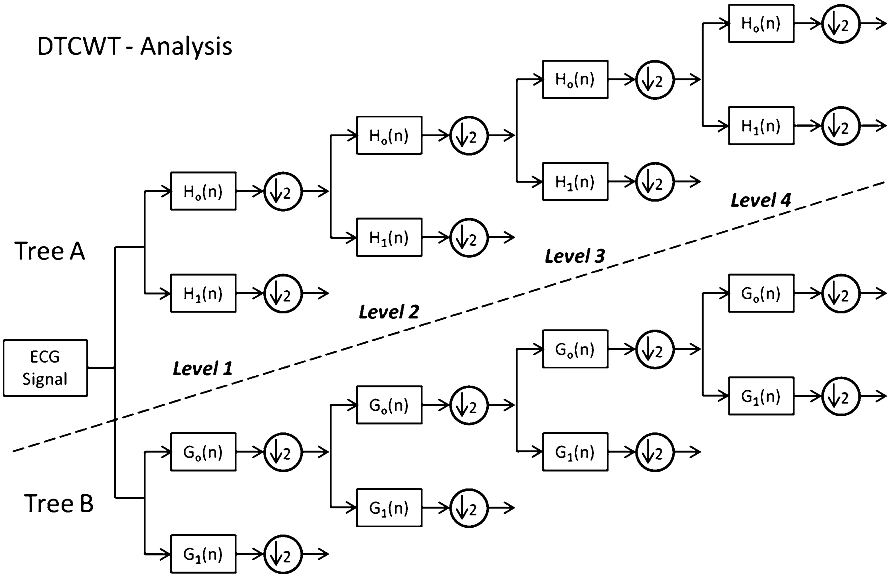

Fig. 7.3 H_0(n) and H_1(n) are, respectively, representatives of high-pass and low-pass filters for tree A. G_0(n) and G_1(n) are high- and low-pass filters for tree B, similarly. The input signal is down sampled to approximately half its original size at each level of decomposition. The output of each level is the detailed and approximation coefficient of the input signal [1]

The coefficients of DT-CWT are calculated as provided below:

$$d_l^C(k) = d_l^{Re}(k) + jd_l^{Im}(k),\ l = 1,\dots,j \tag{5}$$

$$c_j^C(k) = c_j^{Re}(k) + jc_j^{Im}(k) \tag{6}$$

Feature Extraction in DT-CWT

The real and imaginary coefficients from the DT-CWT decomposition and the real part of the approximation coefficient are used to extract features. Five levels of DT-CWT are performed on the ECG signal for windows of length 10 s. For each level, real and complex detailed coefficients as well as the real parts of the level 5 approximate coefficient are considered.

Having $x_1, x_2, \cdots, x_n$ as the values of each coefficient obtained from each 10 s window, several statistical features such as standard deviation, median, minimum and maximum, energy, power, entropy, skewness, kurtosis, range, signal complexity, signal mobility, log of variance, mean of frequencies, variance of probability distribution, sum of autocorrelation, mean of auto-covariance, and entropy of frequency are calculated. Below a brief description of skewness and kurtosis, two statistical features affecting the shape of a signal, is provided.

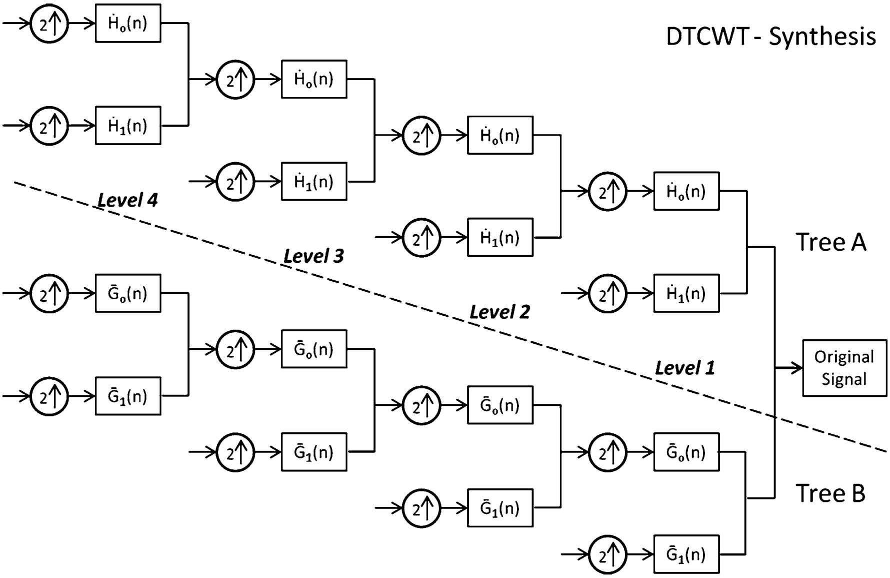

Fig. 7.4 $\dot{\mathbf{H}}_{0(\mathrm{n})}$ and $\dot{\mathbf{H}}_{1(\mathrm{n})}$ are, respectively, representatives of high-pass and low-pass filters for tree A. $\bar{\mathbf{G}}_{0(\mathrm{n})}$ and $\bar{\mathbf{G}}_{1(\mathrm{n})}$ are high- and low-pass filters for tree B. The input signal is down sampled to roughly half its original size at each level of decomposition [1]

Skewness and Kurtosis

Shape parameters are considered as parameters affecting the shape of a distribution as opposed to its location and scale. Skewness and kurtosis are shape parameters measuring the degree of asymmetry and peakedness of the probability distributions, respectively.

Mathematically speaking, skewness gives the third moment of a random variable as shown in (7):

$$Skewness = \frac{\frac{1}{n}\sum_{i=1}^{n}(x_i - \bar{x})^3}{\left[\sqrt{\frac{1}{n}\sum_{i=1}^{n}(x_i - \bar{x})^2}\right]^3} \tag{7}$$

Negative value for skewness represents a probability distribution skewed to the left tail (left of the mean), and positive value demonstrates a distribution skewed more to the right tail (right of the mean).

With kurtosis, the fourth moment of a random variable is provided, as given in (8):

$$Kurtosis = \frac{\frac{1}{n}\sum_{i=1}^{n}(x_i - \bar{x})^4}{\left[\frac{1}{n}\sum_{i=1}^{n}(x_i - \bar{x})^2\right]^2} \tag{8}$$

A distribution concentrated around the mean has a high, sharp peak with a kurtosis value of greater than 3. In contrast, a kurtosis value of less than 3 portrays a flat distribution with low, less obvious peak. Value of 3 is the kurtosis of a normal distribution used as a reference standard.

In the attention detection decision-making computer system by [3], the feature selection process resulted in selecting skewness for all levels of the imaginary parts of the detailed coefficients and levels 1, 3, and 5 of real parts of the detailed coefficients. For kurtosis, level 5 of the approximate coefficient along with levels 4 and 5 of the imaginary part of the detailed coefficient was selected.

Traumatic Brain Injury

Each year, over 1.4 million people in the United States suffer from traumatic brain injury (TBI) [6]. Over 50,000 of these victims do not survive, out of which 50% die in the first two hours after the injury. Hence, it is vital to be able to diagnose the injury quickly. Here, computer tomography (CT) imaging, a fast and economical medical scan, comes handy as the gold standard for initial TBI assessment. Another advantage of CT is that it is capable of uncovering fractures or hematomas.

Increased intracranial pressure (ICP) is a common cause of death and a major complication of TBI which results in deformation of brain tissue. Cranial trepanation is the current method of ICP assessment which can result in patients' bleeding and infection due to its highly invasive nature. Therefore, a noninvasive approach as a preliminary step to perform trepanation would be more preferred.

Changes in the location and size of the ventricles can be helpful in deciding whether to perform cranial trepanation, and these changes are detectable by CT scan. The solution proposed by [6] focuses on automatic processing of CT images of brain for segmentation and identification of the ventricular systems. Segmentation of the ventricles helps in providing vital diagnosis knowledge through measuring the changes in the location and size of the ventricles.

Key features are extracted from CT ventricular images via image processing. The features include the extent of midline shift (a normal midline shift is defined according to the skull symmetry and anatomical features of a normal subject) in the brain and the size of the lateral ventricles.

An ideal midline detection algorithm proposed in [6] consists of the following three steps:

- Approximate midline detection based on the symmetry of the skull
- Falx cerebri and anterior bone protrusion detection
- Midline position refinement using these features

This algorithm resulted in 90% accuracy in midline detection.

A two-step approach is taken for segmentation of the ventricles. The first step is a low-level segmentation on each pixel of the CT images. Iterated conditional mode (ICM) and maximum A posteriori spatial probability (MASP) are the two algorithms used in this step. Comparing the results of these algorithms, ICM with K-means as the initial segmentation method resulted in smoother segmentation, although some small parts were missing. MASP resulted in more noise than ICM. A modified version of MASP is used which speeds up the segmentation process for each slice by dealing only with each pixel's current estimated neighborhood. The comparison is illustrated in Fig. 7.5. In the next step, template matching algorithm is used to isolate the ventricles. The CT dataset used for ventricle segmentation contains mild and severe TBI subjects. In all the cases, the ventricles are detected successfully in all CT slices (100% accuracy).

Pelvic Fracture Detection

One of the most severe types of injuries suffered by trauma patients is traumatic pelvic injuries. Traumatic pelvic injuries along with the associated complications, specifically, hemorrhage and infected hematomas account for 8.6% to 50% of the mortalities. A computer-aided system is required to accelerate the decision-making procedure by analyzing large datasets of patients' information.

The computer-assisted decision-making system proposed in [14] allows for detection of fracture and hemorrhage through processing of CT images to assess the severity of a pelvic injury. A hierarchal procedure, capable of combining image enhancement and segmentation approaches, is proposed which results in accurate bone segmentation.

The procedure starts with detecting the bone regions and applying histogram equalization to the area for achieving a better contrast. To enhance the favorable features in the area, speckle reducing anisotropic diffusion (SRAD) is performed. Finally, with the aid of automated seeded region growing, the initial bone segmentation is refined. In 83% of the cases, the detected contours were acceptably accurate. Figure 7.6 represents the performance of the proposed approach compared to the actual image.

Conclusion

Nowadays, signal processing and machine learning techniques play a major role in dealing with biomedical problems. The noninvasive and computerized solutions these techniques provide to health care environments have increased their popularity and made them reliable tools for addressing medical issues.

In this chapter, two medical problems, hemorrhage detection in traumatic injuries and attention detection using ECG and EEG analysis, have been discussed. Error-correcting output codes (ECOC) and dual-tree complex wavelet transform (DT-CWT) are explained as two machine learning and signal processing techniques,

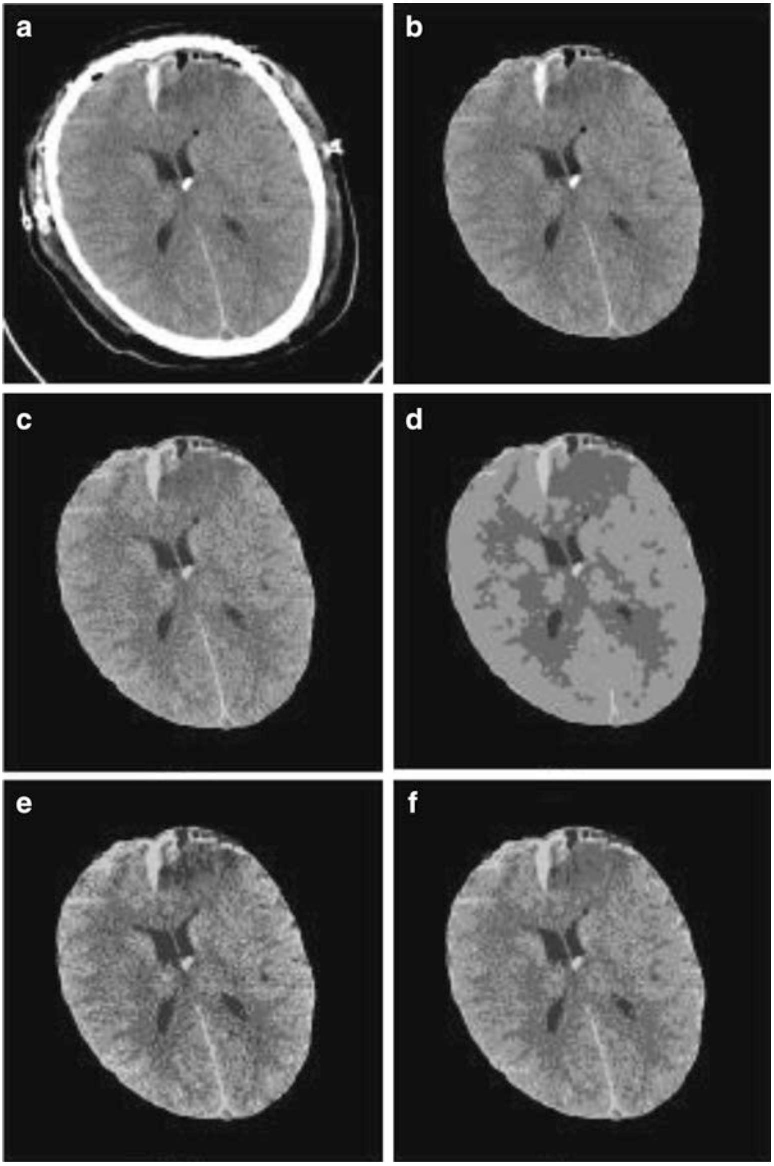

Fig. 7.5 Comparing segmentation methods. (**a**) Actual CT image. (**b**) CT image without the skull. (**c**) Result of K-means algorithm. Four clusters are identified with initial seeds. Noise and uneven intensity distribution have created some holes in the segmentation. (**d**) ICM segmentation with K-means as initial result. ICM gives smoother segmentation, although some small parts are missing. (**e**) MASP segmentation. MASP has resulted in more noise compared to ICM (*the right upper corner* is labeled wrongly as part of ventricles). (**f**) Modified MASP segmentation which is not as smooth as ICP, but resulted in less noise than MASP [6]

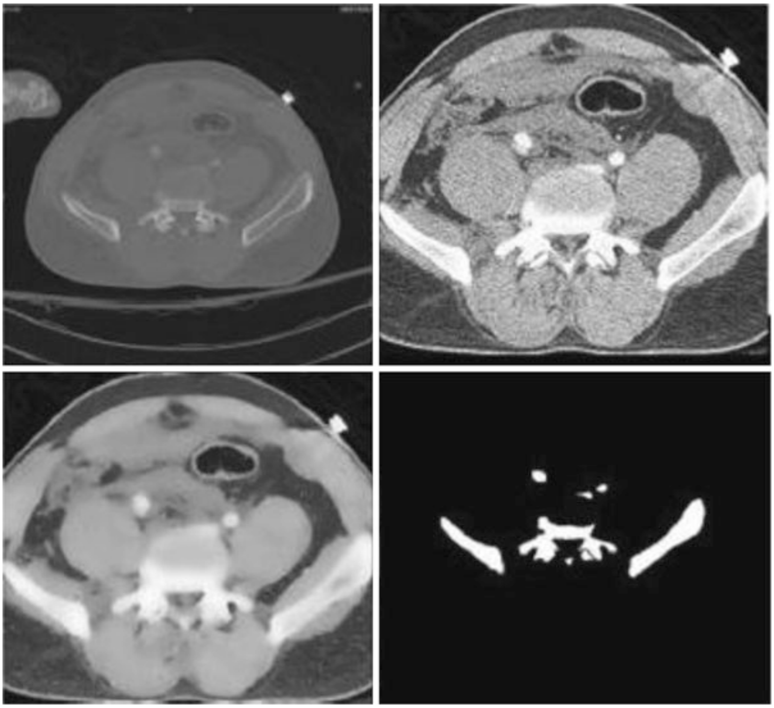

Fig. 7.6 The actual image can be seen in the *upper left corner*. The *upper right corner* represents the region where bone is detected after histogram equalization. The *lower left corner* image shows the image after SRAD filtering. In the *lower right corner*, the segmentation results are provided. The bone contour and shape of the segmented image match with those of the actual image [14]

respectively. Finally, the role of skewness and kurtosis as two statistical parameters for extracting features from DT-CWT has also been discussed.

Traumatic brain and pelvic injuries are investigated using image processing techniques on CT images. Segmentation methods such as ICP and MASP are used to address low-level segmentation on each pixel of the brain CT slices. In the next step, ventricles are detected using template matching algorithm. For pelvic images, a hierarchical procedure merging filtering and histogram equalization is proposed to enhance segmentation quality of the CT images.

Acknowledgement The authors would like to acknowledge Dr. Ashwin Belle, Dr. Yurong Lue, Dr. Simina Vascilache, and Dr. Wenan Chen for contributing their research to this chapter.

References

1. Belle, A.: A Physiological Signal Processing System for Optimal Engagement and Attention Detection (Unpublished doctoral dissertation). Virginia Commonwealth University, Richmond, VA (2012)
2. Belle, A., Hobson Hargraves, R., Najarian, K.: A physiologica signal processing system for optimal engagement and attention detection. In: Proceedings of the IEEE International Conference on Bioinformatics & Biomedicine Workshops, Atlanta, GA., Nov. 12–15, 2011, pp. 555–561
3. Belle, A., Hobson Hargraves, R., Najarian, K.: An automated optimal engagement and attention detection system using electrocardiogram. J. Comput. Math. Meth. Med. (2012). doi:10.1155/2012/528781
4. Belle, A., Ji, S.Y., Ansari, S., Hakimzadeh, R., Ward, K.R., Najarian, K.: Frustration detection with electrocardiogram signal using wavelet transform. In: Proceedings of the International Conference on Biosciences, Cancun, Mexico, Mar. 7–13, 2010, pp. 91–94
5. Belle, A., Pfaffenberger, M., Hobson Hargraves, R., Najarian, K.: An automated decision making system for detecting loss of attention in individuals using real time processing of electroencephalogram. In: Biosignal Interpretation- 7th International Workshop (2012)
6. Chen, W., Smith, R., Ji, S.-Y., Ward, K.R., Najarian, K.: Automated ventricular systems segmentation in brain CT images by combining low-level segmentation and high level template matching. BMC Med. Informat. Decis. Making 9, S4 (2009)
7. Choi, H., Romberg, J., Baraniuk, R., Kingsbury, N.: Hidden markov tree modeling of complex wavelet transforms. In: Proceedings of the IEEE International Conference of Acoustics, Speech, Signal Process, Istanbul, Turkey, June 2000, pp. 133–136
8. Dietterich, T.G., Bakiri, G.: Solving multiclass learning problems via error-correcting output codes. J. Artif. Intell. Res. **2**, 263–286 (1995)
9. Kingsbury, N.G.: The dual-tree complex wavelet transform: A new technique for shift invariance and directional filters. In: Proceedings 8th IEEE DSP Workshop, Utah, Aug. 9–12, 1998
10. Luo, Y.: The Severity of Stages Estimation During Hemorrhage Using Error Correcting Output Codes Method (Unpublished doctoral dissertation). Virginia Commonwealth University, Richmond, VA (2012)
11. Luo, Y., Najarian, K.: Employing decoding of specific error correcting codes as a new classification criterion in multiclass learning problems. In: 2010 International Conference on Pattern Recognition, 2010, pp. 4238–4241
12. Romberg, J., Choi, H., Baraniuk, R.: Multiscale classification using complex wavelets and hidden markov tree models. In: Proceedings of IEEE International Conference on Image Processing, Vancouver, Canada, September 2000. pp. 371–374
13. Selesnick, I., Baraniuk, R., Kingsbury, N.: The dual-tree complex wavelet transform. IEEE Signal Process. Mag. **22**, 123–151 (2005)
14. Vasilache, S., Ward, K., Najarian, K.: Unified wavelet and Gaussian filtering for segmentation of CT images; application in segmentation of bone in pelvic CT images. BMC Med. Informat. Decis. Making **9**, S8 (2009)
15. Wicker, S.B.: Error Control Systems for Digital Communication and Storage. Prentice-Hall, Englewood Cliffs, NJ (1995)